Original Paper

Eletrônica de Potência
Open Journal of Power Electronics

Received July 31, 2024; accepted October 29, 2024; Date of publication November 25, 2024.
The review of this paper was arranged by Associate Editor Montiê A. Vitorino and Editor-in-Chief Heverton A. Pereira.

Digital Object Identifier http://doi.org/10.18618/REP.e202450

Use of Sensorless BLDC Motors for the Hydraulic Power Unit of an Oil Pipeline Inspection Robot

Leonardo F. P. M. Martins[1], Sebastian M. G. Martins[1], Anselmo L. Silva Jr.[1], Augusto P. Souza[1], Bruno R. Santos[1], Fabrízio P. Maziero[1], Luís F. Oliveira[1], Victor B. Coch[1], Elsio Varela[1], Hugo F. L. Santos[2].

[1]SENAI Innovation Institute for Embedded Systems, Florianópolis - SC, Brazil.
[2]Petrobras S/A, Rio de Janeiro - RJ, Brazil.

e-mail: leonardo.malta@sc.senai.br; sebastian.martins@sc.senai.br; anselmo.silva@sc.senai.br; augusto.parigot@sc.senai.br; bruno.rs@sc.senai.br; fabrizio.maziero@sc.senai.br; luis.fernando@sc.senai.br; victor.coch@sc.senai.br; elsio.varela@sc.senai.br; h.santos@petrobras.com.br.

ABSTRACT The challenges encountered in the oil and gas industry require complex solutions and development effort. Related to oil lifting and gathering, it concerns severe conditions as space restraints. Given the confined space inside oil pipelines, robots for inspection requires technologies compatible with it, increasing its complexity, where the minimum required and maximum effective components of the robot is crucial for its construction. In this scenario, the use of sensorless BLDC motors becomes a key point, increasing robustness and reducing harness, being important factors in terms of feasibility, due to connector limitations. Thus, the more motors used — which contributes to the robot's movement — the more advantageous this approach becomes, considering that there is no need for sensing signals for controlling. This work presents an extended version of a paper published on COBEP/SPEC 2023, with new achievements: development of a baseboard motor controller, using TMS320F28027F MCU and DRV8353RSRGZR driver; practical results for sensorless controlling motor; hardware thermal analysis. As results, considering the set point of 5000 rpm rotation speed and a load pressure of 300 bar, the control system obtained a maximum error of 2%.

KEYWORDS sensorless motor control, long oil pipelines, inspection robot, oil and gas industry.

I. INTRODUCTION

The existence of different energy sources, both renewable (e.g. wind and solar) and non-renewable — as know as fossil fuels (e.g. oil, coal and natural gas) — provides a plurality in the process of exploiting and technologies usage. When comparing both types of energy sources, fossil fuels have a higher energy production capacity, with no variations in supply throughout the day. They can also be easily stored in its natural form. On the other hand, solar and wind power are unlimited and give a positive return in terms of environmental protection [1].

Non-renewable sources are more exploited than the renewable ones, even with the popularity of solar and wind powers over the last few years. The greater the global demand for energy, the greater the need to exploit both renewable and non-renewable sources. For context, Figure 1 shows energy production by different sources from 1990 to 2021 in TJ. It can be seen that fossil fuels, led by crude oil, still account for the majority of world production. By the end of 2024, world oil demand is expected to increase by 1.1 mb/d, while the outlook for 2025 is to increase by 1.2 mb/d, maintaining a stable variation [2].

Accompanied by total energy production, the consumption of oil-based products also tops the list from 1990 to 2021,

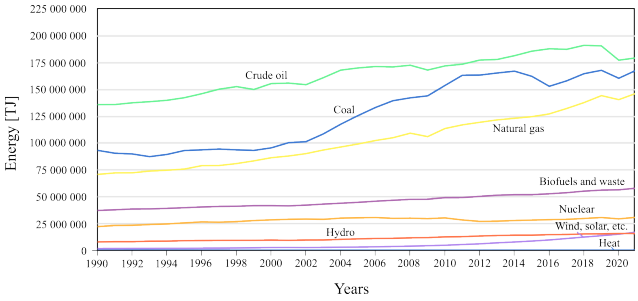

FIGURE 1. Domestic energy production by source, World, 1990-2021 [3].

as can be seen in Figure 2. Many products used worldwide are still characterized by the use of oil, such as gasoline, diesel oil and aviation kerosene. This global consumption increases every year, but in smaller proportions compared to previous decades, precisely because of the advance of renewable energies, mainly related to the concern of nations to protect the environment [2].

However, many problems accompany the oil and gas exploration process, hindering its flow and productivity. One of the main problems encountered during the process through submerged pipelines is the possibility of paraffin and hydrate formation, as can be seen in [4]. There are four main factors

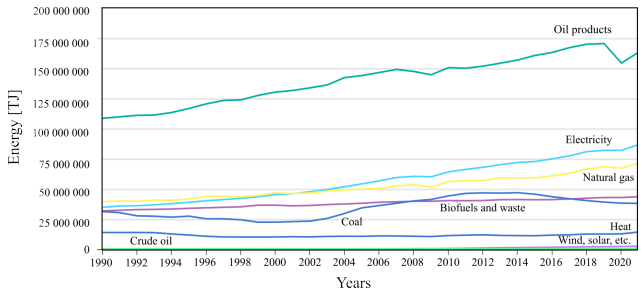

FIGURE 2. Total final consumption (TFC) by source, World, 1990-2021 [3].

that, combined, cause this problem: at the bottom of the sea, few kilometers from the surface, it can be found low temperatures, high pressure, presence of water vapor and hydrocarbons [5]. This eventually leads to an obstruction of the pipeline, making the oil and gas flow process unfeasible.

Some solutions have been tested over the years. One of them, called PIG (pipeline inspection gauge) depends on the pipeline flow and regularly gets stuck inside of it. Remove a stuck PIG can make the unclogging mission even more difficult than just the presence of paraffin and hydrates, therefore leading to risky interventions [6] [7]. Figure 3 shows a representation of a PIG stuck.

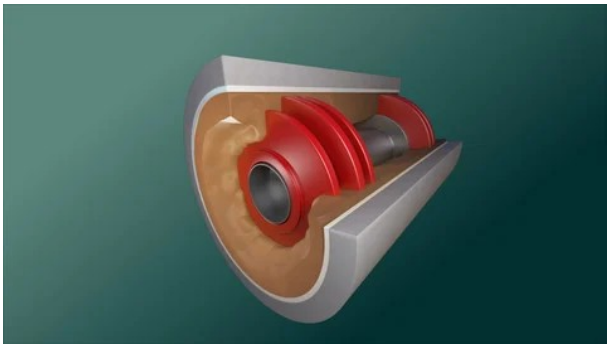

FIGURE 3. Representation of a PIG stuck inside a pipeline [8].

Looking for a solution that reaches long distances, as well as being able to use chemical components for unclogging process, an inspection robot is under development that can identify the obstruction using a sensor located at the tip of it.

This paper is an extended version of [9] and focuses on the development of proprietary baseboard, based on TMS320F28027F MCU and DRV8353RSRGZR driver, for controlling the sensorless motors used in the robot as part of the hydraulic power unit (HPU). The main difference between papers is the use of the designed hardware, instead of a development kit, for experimentation in the laboratory and subsequent assembly inside the robot's pressure vessels. Experimental results, considering different scenarios, shows the capability of the designed controller by obtaining a maximum error of 2% at a target speed of 5000 rpm and pressure load of 300 bar. By way of comparison, with due regard for the target speed, the results in [9] shows a maximum error of almost 9%, considering 6000 rpm and 250 bar pressure.

The previous solution for the HPU considered five BLDC (brushless direct current) motors driven by sensored control. This system is based on hall effect sensors to detect the rotor's position. In applications where precise position or timing is crucial, such as robotic manipulators, sensored control is frequently preferred [10]. Otherwise, the inclusion of sensors does add to overall cost and complexity of motor design and also introduce point of failure, in general caused by the several number of connections - which increases with the number of motors that are positioned inside the HPU.

Removing hall sensors reduces the cost of the system, as fewer components represent easier installation and reduced wiring complexity [11]. Therefore, the motor assembling can be more compact, fitting into constrict spaces. The instability of the control at low speeds and high pressure load is one of the disadvantages for this solution. However, the motors aim to start with no load, maintaining high speed during the robot's movement.

Following sections concern: section II presents the robot architecture, identifying its electronics modules, hydraulic power unit for pumping and moving the robot aided by grip modules, as well as auxiliary tools for unclogging. Electrical and data connection system via umbilical cable are presented as well; section III considers the sensorless BLDC control with the baseboard designed; section IV shows experimental results with graphical visualization and tables indicating control error data in different scenarios; section V is responsible for conclusion and future work.

II. ROBOT ARCHITECTURE

Considering the problems caused by the obstruction of paraffin and hydrates during the oil lift and gathering process, specially generating high operating costs, either caused by the interruption of oil production, many techniques are used in an attempt to unclog the pipes [12]. An alternative solution, under development, is a robot connected by an umbilical cable which moves to the point of obstruction using a gripping system inside the oil pipeline. When the robot meets the obstruction, it will perform the unclogging procedure using a chemical solution, releasing the oil passage. Figure 4 shows the concept for a pipeline unclogging operation using the inspection robot. The robot is inserted into the pipeline with the aid of a launch system, enabling it to be moved using the traction system and find the obstruction [12].

The robot under development, which architecture can be seen in Figure 5, is composed by six main structures:

1) Umbilical Cable: responsible for delivering power and communication to the robot, and also allowing the injection of unclogging solvents;
2) Electronic Devices: the robot system consists of 18 boards with different functions as power conversion, current and voltage sensing, solenoids and motors driving, locomotion state machine controlling, and overall

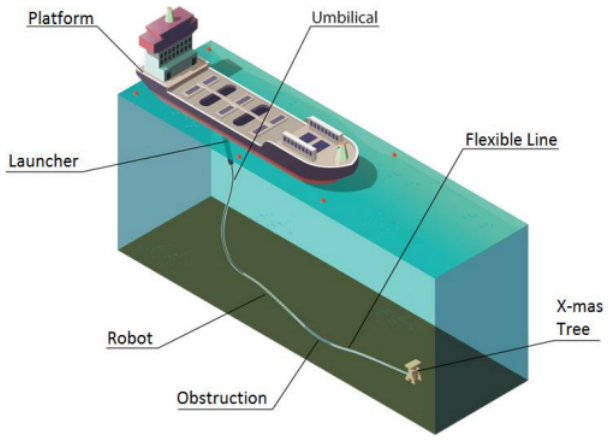

FIGURE 4. Operation concept for the inspection robot unclogging process [12].

robot management by a single board computer (SBC). Each one described at Table 1;

3) Pressure Vessels: responsible for protecting the electronic devices from the hazardous environment inside the pipeline, with high pressure, petroleum, radioactive gases, and explosive atmosphere. The pressure vessels can withstand up to 700 bar of pressure and are chemically resistant;
4) Hydraulic Power Unit: responsible for providing hydraulic power to the robot's locomotion system, composed by brushless motors, swash plate piston pumps, and solenoid valves;
5) Power Train: the robot has two power trains (one for forward and one for backward movement), where each one has two grip modules and a hydraulic actuator. The robot's motion mechanism was inspired by the inchworm movement - an inchworm is an animal that moves through peristalsis and rely on friction to transmit motion [13].
6) Unclogging tool: located at the tip of the robot, the unclogging tool is responsible for injecting solvents into the obstructions, dissolving them and restoring oil flow.

TABLE 1. Electronic devices from the robot.

Board	Functionality
Protection board	Over voltage and protection circuit
Single-board computer	Enables data traffic and processing
Non-regulated converter	Converts 700 V DC to 40 V DC
Regulated converter	Provides a stable 48 V DC bus
Motor controller	Drives the brushless motors
Sensing board	Reads the sensors inside the robot HPU
Drive board	Drives solenoid valves inside the robot HPU
Grip module board	Sense the position of the grip module's pads
Heating tool	Heats the fluid to unclog the obstruction

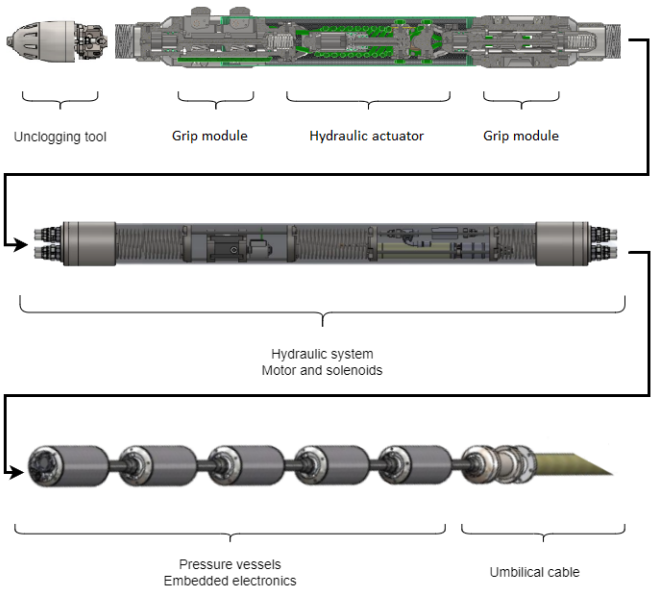

FIGURE 5. Robot architecture adapted from [9].

The designed power electronics can provide up to 4 kW for the motors — and for the rest of the robot — to operate the hydraulic system. The motors are responsible for pressurizing the system's hydraulic line and the grip modules, enabling it to attach the risers' inside walls. Figure 6 shows a representation of the grip modules with its hydraulic actuator inside a pipe.

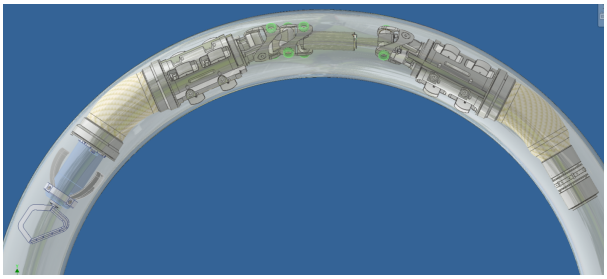

FIGURE 6. Robot movement system using grip modules and an linear hydraulic actuator.

As a data hub, an on-board computer is responsible for maintaining the fiber optic connection with the control room on the platform's surface and directing sensing and control data from a CAN bus, allowing the connection with the rest of electronic boards — called by end devices — including the ones responsible for motor control.

The motors and their respective electrical/signal connections are located inside the HPU, as can be seen in Figure 5. Considering the current solution, a total of five BLDC motors are used for robot movement, each with a three-phase power supply common to all and no use of sensor hall for feedback controlling.

III. SENSORLESS BLDC MOTOR CONTROL

BLDC motor is one of the most widely used motors for industrial applications. According to [14], it is predicted that by 2030, this type of motor will become the main component for power transmission scenarios, surpassing induction motors. The motor used in this project is the EC-4pole-32, from Maxon Group. Figure 7 presents the motor and Table 2 shows its main parameters.

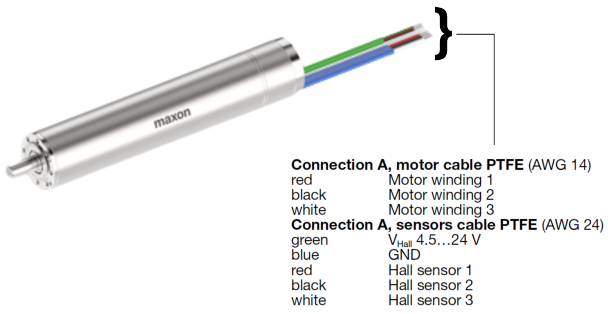

FIGURE 7. BLDC motor used in the pumping system for robot movement [15].

TABLE 2. General parameters at nominal voltage [15].

Parameter	Value
Nominal voltage	48 V
No load speed	6420 rpm
Nominal speed	4670 rpm
Maximum efficiency	82%
IQ full scale frequency	800 Hz
Pole pairs	2
Maximum current	15 A
Flux estimation frequency	20 Hz

In BLDC motors, there is a direct relationship between voltage and speed: the motor speed is proportional to the applied voltage. This means that increasing the voltage will increase the motor speed. Conversely, the relationship between torque and current is also direct: the torque generated by the motor is proportional to the current flowing through the motor's windings. At low speeds, the BLDC motor requires an increase in current to maintain the necessary torque to overcome inertia and external loads. This is because the motor-generated voltage (back-EMF) is lower at low speeds, requiring higher current to produce the same level of torque. This increase in current at low speeds can result in higher energy consumption and heating, which must be managed properly to avoid damage to the motor and the controller.

A broad spectrum of methodologies exists for implementing speed and position control in BLDC motors. Typically, the hall effect sensor method is the preferred approach; however, numerous studies in the literature explore sensorless control, as evidenced in [16]. Sensorless control offers several advantages over sensored systems, including the elimination of physical sensors, which results in reduced cost and simplified maintenance.

Sensorless control of BLDC motors relies on detecting the voltage generated by the motor, known as back-EMF, to determine the rotor position and adjust the commutation of the windings accordingly. Back-EMF is proportional to the motor speed, and at high speeds, the generated voltage is sufficient for precise detection, allowing efficient motor control. However, at low speeds, back-EMF is significantly reduced, making rotor position detection less accurate and challenging for sensorless control. As a result, the system may struggle to maintain proper commutation and desired torque. To compensate, the controller may increase the current, which helps maintain torque but can also lead to higher energy consumption and heating.

Considering the robot structure illustrated in section II, and the motor's connections in Figure 7, the comparison between hall sensor and sensorless control methods underscores a significant difference in cable management. In a robot with five motors, each motor has three phase cables and five hall sensor cables, which are categorized as follows: three cables for hall sensor signals (one for each sensing function) and two cables for powering the sensors. This results in a high pin count and complex cabling. Specifically, with hall sensors, the total number of pins required amounts to 42 — comprising 15 phase cables (3 per motor), 15 Hall sensor signal cables (3 per motor), and 10 sensor power cables (2 per motor).

In contrast, sensorless control eliminates the need for hall sensor cables, which simplifies the wiring significantly. By utilizing commercial connectors, the number of pins is reduced from 42 to 25 — representing approximately a 60% reduction. This substantial gain not only simplifies the wiring but also enhances robustness and maintainability, effectively addressing the constraints imposed by the limited internal space within the robot.

Considering the advantages presented above, a sensorless control based on Clarke and Park transforms with the Field Oriented Control (FOC) is implemented. Clarke and Park transforms are used in high performance drive architectures, while FOC is a method for variable frequency control of the stator in a motor drive [17].

The hardware designed for driving Maxon's three-phase BLDC motors incorporates the DRV8353RSRGZR, a three-phase smart gate driver that provides high-precision control and includes current amplifiers, peak current control, overcurrent and overvoltage protection, as well as an integrated voltage regulator. Operating within a 9 V to 75 V input range, it uses a constant on-time (COT) mode for fixed-frequency operation, reducing the need for external components.

The system features a baseboard containing the TMS320F28027F microcontroller that executes motor control algorithms, including InstaSPIN, and generates PWM signals for MOSFET control. To handle CAN communication, the STM32F091RCT6 is used for CAN to

UART conversion, while a digital isolator ensures signal integrity between the PWM signals and the driver. The simplified schematic is presented in Figure 8, and the hardware developed is presented in Figure 9.

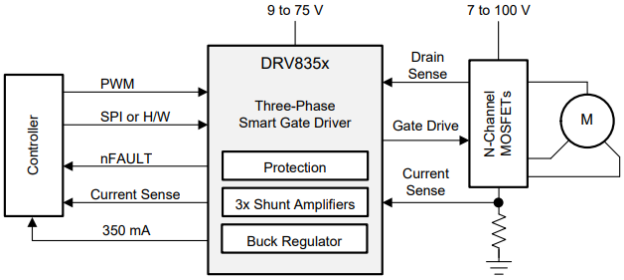

FIGURE 8. Simplified schematic for DRV835x Gate Driver [18].

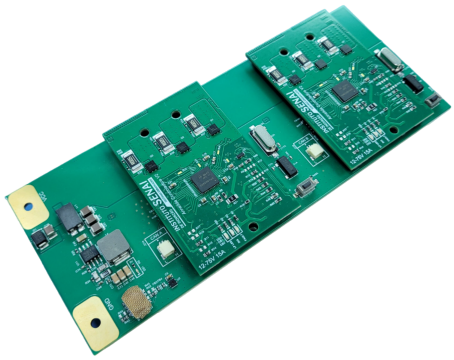

FIGURE 9. Sensorless control hardware developed.

Main features for Sensorless control hardware are presented below:

- 9 to 75 V operation;
- 15 A continuous / 20 A peak H-bridge output current;
- Internal buck regulator;
- Three individual, internal low-side current shunt amplifiers;
- InstaSPIN-FOC firmware available.

Each baseboard is capable of supporting the connection of two motor controllers per PCB, allowing for the control of two motors within a single pressure vessel of the robot. This design streamlines the system by reducing the number of PCBs required and enhances the overall efficiency and compactness of the robot's internal structure. By enabling dual motor control within one pressure vessel, it optimizes space utilization and simplifies the wiring and maintenance processes, contributing to a more robust and maintainable robotic system.

The developed system enables a sensorless solution that can identify, tune the torque controller and efficiently control the motor. Using an unified observer structure known as FAST (Flux, flux Angle, motor shaft Speed and Torque), the system identifies required motor parameters and provides feedback signals [19]. Based on these estimated parameters, the gains of two control loops — current and speed — for a PI controller are calculated. Experimental results can be seen in section IV, presenting the system's control capacity for different pressurization scenarios in an oil tank simulating the robot's hydraulic reservoir.

IV. EXPERIMENTAL RESULTS

The bench tests aim to validate the hardware developed for controlling sensorless BLDC motors, focusing on its application within the actual robot framework. The tests were designed to ensure that the hardware meets the necessary performance, efficiency, and robustness requirements for its integration into the robotic system.

A BLDC motor was used immersed in an oil tank, connected to a solenoid valve and a manifold manometer as part of the test environment, represented in Figure 10 — reused figure from [9] that characterizes the same environment as the tests carried out and presented in the current research for motor controlling.

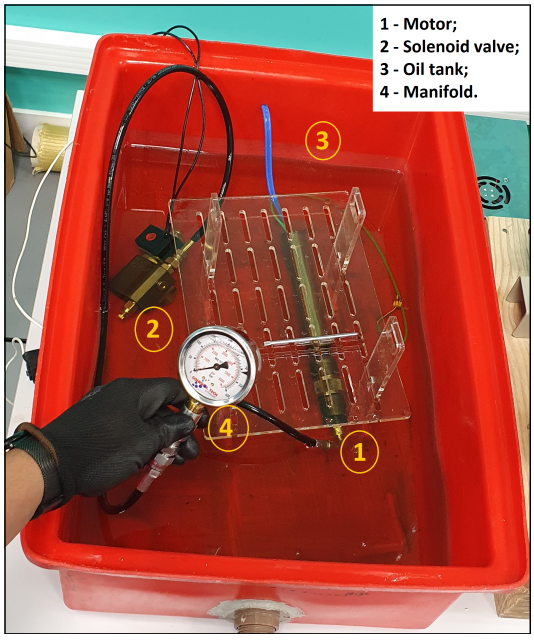

FIGURE 10. Motor immersed in oil tank [9].

The developed electronics board is housed within a pressure vessel, as illustrated in Figure 11. This encapsulation system is designed to protect the electronic components from high environmental pressures, which can reach up to 300 bar. By maintaining a controlled internal environment, the pressure vessel ensures the reliability and longevity of the electronic system. This protective measure is particularly important given the robot's operational requirements, including long distances (up to 15,000 m), high friction forces along the umbilical cable, the small internal diameter of flexible lines (4 and 6 inches), the necessity to navigate curves, and the challenges of remote operation such as communication latency and load loss.

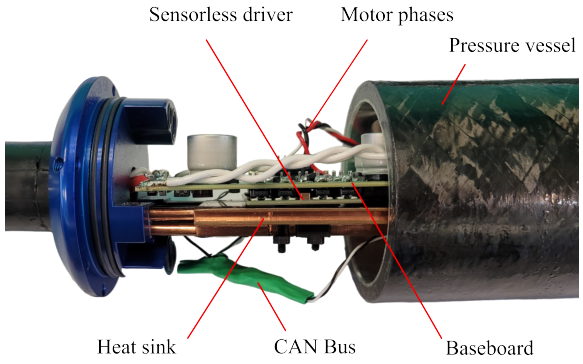

FIGURE 11. Sensorless controller embedded system.

Motor's parameters values can be seen in Table 3, as the controller parameters in Table 4 where L_{s-d} and L_{s-q} are the stator inductance, Rated Flux is the identified total flux linkage between the rotor and the stator and R_s is the phase to neutral resistance — these estimated parameters are based on the motor parameters; while K_p and K_i are the proportional and integral gains of speed and current loops — these gains are based on the estimated parameters.

TABLE 3. Motor parameters.

Parameter	Value
L_{s-d}	0.06343 mH
L_{s-q}	0.06343 mH
Rated Flux	0.14225 V/Hz
R_s	0.27184 Ω

TABLE 4. Controller gains.

Gain	Value
K_p (speed)	10.00
K_i (speed)	0.0667
K_p (current)	0.08
K_i (current)	0.9950

A. SPEED CONTROL CAPABILITY

As discussed in the previous subsection, there is a direct relationship between voltage and speed in BLDC motors: the motor speed is proportional to the applied voltage, while the torque is proportional to the current flowing through the motor's windings. Considering this, two main operational scenarios were evaluated for the tests. These scenarios emphasize different aspects of the hardware's performance, particularly its ability to maintain the motor speed at the set point of 5000 rpm. By evaluating the hardware under these conditions, it can reliably control the motor speed and manage energy consumption and heating effectively, confirming its suitability for the robotic system.

- **Scenario 1: 48 V Input Bus**
  - *Objective:* to observe the maintenance of motor rotation for load variations in the hydraulic circuit from 0 to 300 bar.
  - *Procedure:* the BLDC motor was operated with a 48 V input. During the test, the load in the hydraulic circuit was varied from 0 to 300 bar, and the motor rotation was continuously monitored.
- **Scenario 2: 56 V Input Bus**
  - *Objective:* to follow the same test structure as the first scenario but with a 56 V input, to observe the relationship between rotation and voltage in BLDC motors.
  - *Procedure:* the BLDC motor was operated with a 56 V input. The rotation was monitored while the load in the hydraulic circuit varied from 0 to 300 bar.

Figure 12 compares the results of rotation and pressure variation for both scenarios, showing greater stability at the higher voltage. It is observed that, with a 56 V input, the system managed to maintain control of the rotation across the entire pressure range, whereas with 48 V, the control performance was compromised, failing to maintain the rotation at higher pressures.

FIGURE 12. Comparison between scenario 1 and scenario 2.

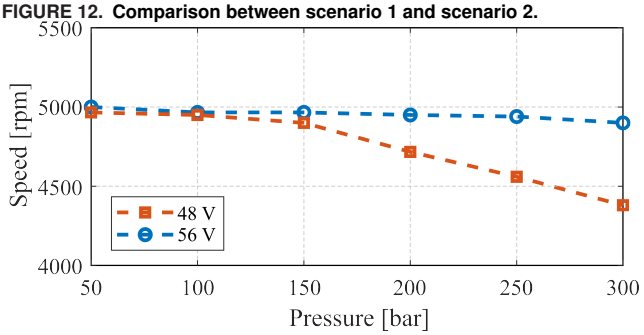

The control error can be seen in Table 5 and Table 6 for both scenarios.

TABLE 5. Experimental results for sensorless motor control - 48 V bus

Pressure	Estimated speed	Absolute error	Error
50 bar	4966 rpm	-34 rpm	-0.68%
100 bar	4950 rpm	-50 rpm	-1%
150 bar	4900 rpm	-100 rpm	-2%
200 bar	4717 rpm	-283 rpm	-5.66%
250 bar	4560 rpm	-440 rpm	-8.8%
300 bar	4380 rpm	-620 rpm	-12.4%

The results from the experimental tests reveal notable differences between the performance of the system with a 56 V input compared to a 48 V input. At 56 V, the system demonstrates relatively low absolute errors across various pressure levels. For instance, at 50 bar, the estimated speed closely matches the target of 5000 rpm with zero error, and

TABLE 6. Experimental results for sensorless motor control - 56 V bus

Pressure	Estimated speed	Absolute error	Error
50 bar	5000 rpm	0 rpm	0%
100 bar	4966 rpm	-34 rpm	-0.68%
150 bar	4960 rpm	-40 rpm	-0.8%
200 bar	4950 rpm	-50 rpm	-1%
250 bar	4940 rpm	-60 rpm	-1.2%
300 bar	4900 rpm	-100 rpm	-2%

even at higher pressures, such as 300 bar, the maximum error is 2%. This indicates a stable and accurate performance of the control system, maintaining good speed regulation across the range of pressures.

In contrast, with a 48 V input, the system shows increased deviations from the target speed as pressure rises. While the error remains manageable at lower pressures, such as 50 bar and 100 bar, with errors of 0.68% and 1% respectively, the performance deteriorates significantly at higher pressures. At 200 bar, the error increases dramatically to 5.66%, and at 300 bar, the system exhibits a substantial error of 12.4%. This suggests that the reduced input voltage impacts the system's ability to maintain precise control, resulting in larger discrepancies between the estimated and target speeds as pressure increases.

Given that the rpm speed of the five-motor set is directly proportional to the effective movement speed of the robot, the observed errors in motor speed translate directly into variations in the robot's actual movement speed. Comparing the two scenarios, the system with a 56 V input maintains relatively minor errors across the pressure range, with a maximum error of 2% at 300 bar. This minor error suggests that the robot's effective movement speed would vary by up to 2% from the target speed. Conversely, with a 48 V input, the system shows significantly larger errors, reaching 12.4% at 300 bar. This substantial error implies that the robot's effective movement speed could deviate by up to 12.4% from the intended speed. Therefore, the higher input voltage not only ensures better motor speed control but also results in a more consistent and accurate effective movement speed of the robot, reducing the potential for performance discrepancies in practical applications.

On the other hand, [9] shows a maximum absolute error of 8.91% for 6000 rpm target speed and 250 bar pressure, indicating a substantial improvement with the new embedded control system acting on the developed baseboard.

B. MOSFETS THERMAL ANALYSIS

One of the main concerns in the design of BLDC motor control systems is the thermal management of electronic components, especially MOSFETs. The increase in temperature of these components can lead to a reduction in system efficiency, component degradation, and even catastrophic failures. Therefore, it is essential to understand the mechanisms that cause MOSFET heating and develop effective methods to predict and mitigate these effects.

The developed hardware employs the NTTFD021N08C MOSFET due to its favorable characteristics for high-performance BLDC motor control systems. This MOSFET offers low on-resistance and high current handling capabilities, making it suitable for applications that require efficient switching and robust thermal performance. The choice of the NTTFD021N08C was influenced by its ability to minimize energy losses and manage heat dissipation effectively, ensuring reliable operation under varying load conditions. Table 7 shows the NTTFD021N08C characteristics.

TABLE 7. Characteristics of the NTTFD021N08C MOSFET

Parameter	Value
Maximum Drain-Source Voltage (V_{DS})	80 V
Continuous Drain Current (I_D) at 25 °C	24 A
Continuous Drain Current (I_D) at 100 °C	15 A
On-Resistance ($R_{DS(on)}$)	21 mΩ
Gate Charge (Q_g)	8.4 nC
Thermal Resistance, Junction to Case ($R_{\theta JC}$)	4.8°C/W
Thermal Resistance, Junction to Ambient ($R_{\theta JC}$)	70°C/W
Operating Temperature Range (T_J)	-55 °C to 150 °C

Thus, the mathematical model presented in [20] is used to predict the thermal behavior of MOSFETs under different operating conditions. This mathematical model considers the values of the gate resistor and gate capacitor inserted into the drive circuit, allowing the evaluation of how the choice of these components impacts the temperature rise of the MOSFETs. Subsequently, this model is compared to experimental bench results, shown in Figure 13. The comparison between the experimental data and the model predictions not only validates the model's accuracy but also provides valuable insights for the improvement of the design and operation of BLDC motor control systems.

FIGURE 13. Thermal response of MOSFETs.

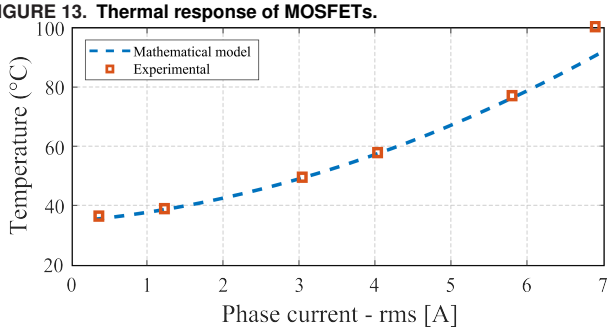

V. CONCLUSION

The validation and performance assessment of the developed hardware for controlling sensorless BLDC motors were carried out through comprehensive bench tests focused on its application within the robot's existing structure, evaluating an extended research for [9]. The tests aimed to ensure

that the hardware met the necessary performance, efficiency, and robustness requirements. The results demonstrated a significant difference in performance between two voltage scenarios: 48 V and 56 V. At 56 V, the system maintained motor speed with minimal error across various pressures, ensuring a maximum error of 2% at 300 bar. Conversely, the 48 V scenario exhibited substantial errors, reaching up to 12.4%, directly impacting the robot's effective movement speed. Additionally, the use of sensorless BLDC motors reduced the complexity and weight of the cabling, contributing to a more streamlined and efficient design.

Moreover, the NTTFD021N08C MOSFET's low on-resistance and high current handling capabilities were crucial for maintaining efficient switching and robust thermal performance, minimizing energy losses and effectively managing heat dissipation. Additionally, the electronics board was housed within a pressure vessel to protect it from high environmental pressures up to 300 bar and other operational challenges, ensuring system longevity and reliability. These findings underscore the importance of adequate voltage supply and protective measures in developing high-performance BLDC motor control systems for robotic applications. The sensorless configuration further enhanced the system by reducing cabling needs, simplifying installation, and lowering maintenance requirements.

These insights provide a foundation for future enhancements in design and operation, leading to improved performance and reliability in practical applications. In addition, for future work, the robot will be tested in a field environment using the proposed solution for sensorless motor control.

ACKNOWLEDGMENT

This work was supported by Brazilian National Agency for Petroleum, Natural Gas and Biofuels (ANP) and National Service of Industrial Apprenticeship of Santa Catarina State (SENAI/SC). The authors are grateful for the partnership in the development of the inspection robot project, in particular to Petrobras S/A, SENAI Innovation Institutes network, represented by Embedded Systems (ISI-SE), Manufacturing Systems (ISI-SM) and Polymeres Engineering (ISI-EP), UpSensor Technology, Federal University of Rio Grande do Sul (UFRGS) and University of São Paulo (USP). The commitment of all participants represents a historic milestone for Brazil, the world and the oil and gas industry.

AUTHOR'S CONTRIBUTIONS

MARTINS, L. F. P. M.: Conceptualization, Data Curation, Formal Analysis, Funding Acquisition, Investigation, Methodology, Project Administration, Software, Supervision, Validation, Visualization, Writing – Original Draft, Writing – Review & Editing. **MARTINS, S. M. G.**: Conceptualization, Data Curation, Formal Analysis, Funding Acquisition, Investigation, Methodology, Software, Validation, Visualization, Writing – Original Draft, Writing – Review & Editing. **SILVA JR., A. L.**: Conceptualization, Data Curation, Formal Analysis, Funding Acquisition, Investigation, Project Administration, Resources, Supervision, Validation, Writing – Original Draft, Writing – Review & Editing. **SOUZA, A. P.**: Data Curation, Funding Acquisition, Validation, Writing – Review & Editing. **SANTOS, B. R.**: Data Curation, Funding Acquisition, Validation. **MAZIERO, F. P.**: Conceptualization, Data Curation, Funding Acquisition, Project Administration, Validation, Writing – Review & Editing. **OLIVEIRA, L. F.**: Data Curation, Formal Analysis, Funding Acquisition, Investigation, Methodology, Software, Validation, Visualization, Writing – Review & Editing. **COCH, V. B.**: Data Curation, Formal Analysis, Funding Acquisition, Validation. **VARELA, E.**: Data Curation, Funding Acquisition, Resources, Validation. **SANTOS, H. F. L.**: Conceptualization, Funding Acquisition, Project Administration, Resources, Supervision, Validation.

PLAGIARISM POLICY

This article was submitted to the similarity system provided by Crossref and powered by iThenticate – Similarity Check.

REFERENCES

[1] D. Maridin, "Advantages and disadvantages of renewable energy sources utilization", *International Journal of Energy Economics and Policy*, pp. 176–183, April 2021, doi:10.32479/ijeep.11027.

[2] *Oil Market Report - May 2024, IEA*, International Energy Agency, May 2024, URL: https://www.iea.org/reports/oil-market-report-may-2024.

[3] *Energy Statistics Data Browser*, International Energy Agency, December 2023, URL: https://www.iea.org/data-and-statistics/data-tools/energy-statistics-data-browser.

[4] J. da S.T. dos Santos, A. C. Fernandes, M. Giulietti, "Study of the paraffin deposit formation using the cold finger methodology for Brazilian crude oils", *Journal of Petroleum Science and Engineering*, vol. 45, no. 1, pp. 47–60, November 2004, doi:10.1016/j.petrol.2004.05.003.

[5] A. Bozorgia, "Investigation of the History of Formation of Gas Hydrates", *Journal of Engineering in Industrial Research*, pp. 1–19, August 2020, doi:10.22034/jeires.2020.260854.1000.

[6] P. Rao, V. Yelgaonkar, C. Tiwari, V. Dhakar, M. Panicker, "Locating block caused by stuck PIGs in multi product pipeline using combination of radioisotope techniques", *Applied Radiation and Isotopes*, vol. 193, p. 110660, March 2023, doi:10.1016/j.apradiso.2023.110660.

[7] C. Ramella, G. Canavese, S. Corbellini, M. Pirola, M. Cocuzza, L. Scaltrito, S. Ferrero, C. Pirri, G. Ghione, V. Rocca, A. Tasso, A. D. Lullo, "A novel smart caliper foam pig for low-cost pipeline inspection – Part B: Field test and data processing", *Journal of Petroleum Science and Engineering*, vol. 133, pp. 771–775, September 2015, doi:10.1016/j.petrol.2014.09.038.

[8] *How quickly find a stuck PIG in your subsea pipeline*, Tracerco, July 2021, URL: https://blog.tracerco.com/marketing/how-to-find-a-stuck-pig-in-your-subsea-pipeline.

[9] L. Martins, et al., "Sensorless BLDC Motor Control for Long Oil Pipelines Inspection Robot", *IEEE 8th Southern Power Electronics Conference and 17th Brazilian Power Electronics Conference*, November 2023, doi:10.1109/SPEC56436.2023.10408171.

[10] T. Nama, A. K. Gogoi, P. Tripathy, "Application of a smart hall effect sensor system for 3-phase BLDC drives", *in 2017 IEEE International Symposium on Robotics and Intelligent Sensors (IRIS)*, pp. 208–212, October 2017, doi:10.1109/IRIS.2017.8250123.

[11] L.-C. Zhu, J.-Y. Huang, M.-Y. Wang, C.-J. Zhou, X.-L. Mao, "Back EMF-Based Sensorless Control of BLDCM", *in 2021 IEEE Sustainable Power and Energy Conference (iSPEC)*, pp. 3382–3386, December 2021, doi:10.1109/iSPEC53008.2021.9736116.

[12] H. Santos, et al., "Proposal and Experimental Trials on a Robot for Hydrate and Paraffin Removal in Submarine Flexible Lines", *in 2020 Offshore Technology Conference*, May 2020, doi:10.4043/30663-MS.
[13] R. Li, et al., "An Inchworm-Like Climbing Robot Based on Cable-Driven Grippers", *IEEE/ASME Transactions on Mechatronics*, pp. 1–10, September 2023, doi:10.1109/TMECH.2023.3307682.
[14] D. Mohanraj, R. Aruldavid, R. Verma, K. Sathiyasekar, A. B. Barnawi, B. Chokkalingam, L. Mihet-Popa, "A Review of BLDC Motor: State of Art, Advanced Control Techniques, and Applications", *IEEE Access*, May 2022, doi:10.1109/ACCESS.2022.3175011.
[15] *EC-4pole 32 brushless, 480 watt: Heavy Duty - for applications in oil*, Maxon Group, March 2021.
[16] J.-C. Gamazo-Real, V. Martínez-Martínez, J. Gomez-Gil, "ANN-based position and speed sensorless estimation for BLDC motors", *Measurement*, January 2022, doi:10.1016/j.measurement.2021.110602.
[17] *Clarke & Park Transforms on the TMS320C2xx*, Texas Instruments.
[18] *DRV835x 100-V Three-Phase Smart Gate Driver*, Texas Instruments, August 2018.
[19] *InstaSPIN-FOC and InstaSPIN-MOTION User's Guide*, Texas Instruments, January 2013.
[20] E. Prado, P. Bolsi, H. Sartori, J. Pinheiro, "Modelo Analítico de Cálculo de Perdas em MOSFETs de Potência para Aplicação em Banco de Dados", *Eletrônica de Potência*, vol. 26, pp. 1–11, December 2021, doi:10.18618/REP.2021.4.0023.

BIOGRAPHIES

Leonardo Ferreira Pacheco Malta Martins received his B.S. degree in Control and Automation Engineering from the Federal Institute of Amazonas in 2018 and his M.S. degree in Automation and Systems Engineering from the Federal University of Santa Catarina in 2021, where he contributed to the renewable energy research group with focus on Airborne Wind Energy. Since 2021, he has been a researcher at the SENAI Innovation Institute for Embedded Systems, leading the institute's firmware team in the development of innovation projects. His current research interests are embedded control algorithms, robotic systems for the oil and gas industry, edge AI and IoT applications.

Sebastian Moreira Gomes Martins received his B.S. degree in Electrical Engineering from the Regional University of Northwestern Rio Grande do Sul in 2016 and his M.S. and Ph.D. degrees in Electrical Engineering from the Federal University of Santa Maria in 2018 and 2024, respectively, carrying out research related to the development of a CC-CC converter applied to LED lighting systems in resonant LLC converters. Since 2022 he has been a hardware researcher at the SENAI Innovation Institute for Embedded Systems. His current research interests are microcontrolled circuit designs, LED lighting drivers, BLDC motors and MPPT circuits for photovoltaic systems.

Anselmo Luis da Silva Junior obtained a Bachelor's degree in Electronic Engineering in 2015 and a Master's degree in 2018, both from the Federal University of Santa Catarina. He has 4 years of experience in the development of analog integrated circuits and modeling of MOS transistors, being part of the team at the Integrated Circuits Laboratory - LCI at UFSC. Since 2015, he has worked as a researcher at the SENAI Innovation Institute for Embedded Systems. He has extensive experience in the development of embedded hardware and leading multidisciplinary teams in complex projects.

Augusto Parigot received his B.S. degree in Mechanical Engineering in 2016 and his M.S. degree in Mechanical Engineering from the Federal University of Santa Catarina in 2024, where he contributed to the Integrated Product Development Laboratory group with focus on Multidisciplinary Product Development and Systems Engineering. Since 2017 he has been a mechanical design researcher at the SENAI Innovation Institute for Embedded Systems, working directly on development of innovation projects. His current research interests are systems engineering, product development and integration, and robotic systems for the oil and gas industry.

Bruno Ribeiro dos Santos received the title of Automation Technician from SENAI in 2014. For three years he has been a laboratory technician at SENAI Innovation Institute for Embedded Systems, with focus on assembling and testing of mechanical and automation systems. He is currently studying Industrial Automation at Unifatecie.

Elsio Varela obtained his Technologist degree in Industrial Mechatronics from Federal Institute of Santa Catarina in 2010. He is currently a researcher at the SENAI Innovation Institute for Manufacturing Systems. He has interest and experience in robotics, assembly and testing of mechanical and automation systems.

Fabrízio Piccoli Maziero received his B.S. degree in Electrical Engineering from University of Passo Fundo in 2014 and his M.S. degree in Electrical Engineering form Federal University of Santa Catarina in 2016, focusing on hardware functional verification for space critical application. He works as a researcher at SENAI Innovation Institute for Embedded Systems since 2016, leading the institute's hardware team in the development of innovation projects. His main areas of work is hardware development for a wide range of applications, from industrial IoT devices, subsea robotics and nanosatellite electronics.

Luís Fernando de Oliveira received his B.S. degree in Machatronics Engineering from Federal Institute of Santa Catarina in 2023. Since 2024, he works as a researcher at SENAI Innovation Institute for Embedded Systems, working on the development of firmware solutions for innovation projects. His current research interests are real-time operating systems for microcontrollers, machine learning and image acquisition and processing.

Victor Barros Coch earned his Bachelor's degree in Automation Engineering from the Federal University of Rio Grande in 2022 and went on to complete a Master's in Computer Engineering there in 2024. During his graduate studies, he contributed to the development of a robotic gait training platform for children with cerebral palsy. Since 2024, he has served as a researcher at the SENAI Innovation Institute for Embedded Systems, where he actively works on innovative projects. His current research interests include control algorithms, embedded systems, and robotic systems for the oil and gas industry.

Hugo Francisco Lisboa Santos received his B.S. degree in Mechanical Engineering from the Military Institute of Engineering (IME) in 2008, graduating as the top student, and his M.S. degree in Robotics from the Pontifical Catholic University of Rio de Janeiro (PUC-Rio) in 2011. He has led and contributed to multiple innovation projects at Petrobras, including Annelida and Robin, focusing on well engineering and robotics. His work has earned him more than 30 awards, including the ANP Innovation Award and multiple Petrobras Inventor Awards. He holds 13 national, and 88 international patents. His current research interests include well engineering, robotic systems, and renewable energy.